Synthesis of Photoluminescence Si Nanoparticles: Size Controlling and Surface Functionalization

Yunzi Xin*, Takashi Shirai**

*Advanced Ceramics Research Center, Nagoya Institute of Technology
Gokiso-cho, Showa-ku, Nagoya, Aichi 466-8555, JAPAN

** Department of Life Science and Applied Chemistry, Graduate School of Engineering,
Nagoya Institute of Technology
Gokiso-cho, Showa-ku, Nagoya, Aichi 466-8555, JAPAN

Si nanoparticle (NP), as one of the most promising functional materials has attracted much attention in next-generation optoelectronic device, photovoltaic and in-vivo/in-vitro bio-imaging technologies, based on its tunable band structure induced optical properties. Due to the quantum confinement effect and large surface to core atom numbers, controlling of size and selective surface passivation during synthesis process, become the most important issue for designing of chemical and physical properties of Si NP. This paper reviews the synthesis method of Si NP with respect to size-controlling and surface functionalization as well as its photoluminescence properties.

Keywords: Si, nanoparticle, photoluminescence, size controlling, surface functionalization

Si nanoparticles (NPs) with quantum confinement effect induced unique electronic structure and optical properties [1-9] hold great promise in application of next-generation optoelectronic device [10-17], photovoltaic [19-24] and *in-vivo* and *in-vitro* bio-imaging [25-29], also by taking advantages of its nature abundance, nontoxicity and biodegradability. By utilizing crystalline Si NPs (Si nanocrystals, Si NCs) as emissive material, F. Maier-Flaig et. al developed multicolor light-emitting diodes (LEDs) which performs orange to red electroluminescence (EL) with the highest external quantum efficiency (EQE) of 1.1 % for red emitter in 2013 [14]. The highest EQE for red region EL achieved to 2.7 %, was further updated later by Pi and Qin's groups by applying an inverted device structure [17]. In 2015, Xin et al. initially reported the white-blue EL from a Si quantum dot (QD) hybrid LED with 77.8 % efficient emission from blue Si QDs, which enables the development of white emissive large-area solid-state lighting technology for next-generation displays [16]. As for photovoltaic applications, Kim et al. reported highly efficient Si NC hetero-junction solar cells recently [18]. Meinardi et al. reported Si NC based highly efficient luminescent solar concentrators, and their flexible device with comparable performance to at concentrators provides new design freedom for building integrated photovoltaic elements [22]. By applying water-soluble Si NPs, Wang et al. reported the effective imaging of living cells with a fluorescence lifetime imaging microscopy [24].

Since the first report on room-temperature photoluminescence (PL) from nano-Si [29], theoretical [8,30-35] and experimental [8,9,30,36-88] studies on photoluminescent Si NPs have been numerously conducted. As for theoretical researches, the investigation of absorption and emission mechanism has been discussed as a function of particle size, based on the simulation of molecular orbital of Si NCs [8,30-35]. In the case of experimental researches, Si NPs have been synthesized by different methods, and their sizes, chemical structures and compositions, as well as optical properties have been extensively studied [8,9,39,36-88]. The PL mechanism of Si NPs has been mainly summarized as the following two origins: (i) intrinsic recombination of electrons and holes based on quantum confined band structure in a core; (ii) extrinsic recombination through an induced level on surface. Therefore, the luminescence from Si NPs is not only dependent of the size of NP core, but also strongly affected by the chemical state on surface. Since the number of Si atoms on surface can reach nearly 50 % of all atoms in a Si NP when its size is reduced to 2 nm, surface chemical state may significantly affect the electronic state of ultra-small Si NP. Thus, size-controlling and surface functionalization enable the material designing through the electronic and optical

properties of Si NPs. It is also worth noting that an effective surface functionalization can also optimize chemical properties of Si NPs, such as solubility in hydrophilic and hydrophobic solvents, which might be important factor towards further applications of Si NPs. Controlling of Si NP size has been achieved by adjusting the experimental conditions during either synthesis or additional size-reducing via chemical etching by hydrofluoric acid. Surface functionalization of various inorganic and organic groups have been induced in both synthesis stage and further chemical reactions on hydrogen-terminated Si NPs.

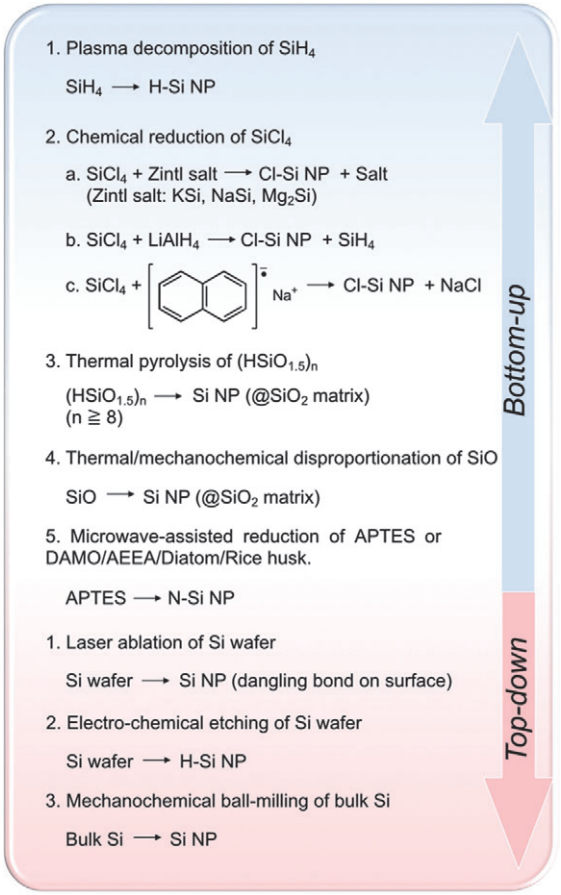

Figure 1. Summary of bottom-up and top-down synthesis methods of Si NPs.

The synthesis process of Si NPs can be categorized as bottom-up and top-down approaches, as summarized in Figure 1. Bottom-up process consists of plasma decomposition of silane (SiH_4) [37-41], chemical reduction of tetrachloride silane ($SiCl_4$) [42-55], thermal pyrolysis of hydrogen silsesquioxane (HSQ) and $(HSiO_{1.5})_n$ (n>8) polymer [56-62], thermal and mechanochemical disproportionation of silicon monoxide (SiO) [63-67], microwave-assisted reduction of (3-aminopropyl) trimethoxysilane (APTES) precursor [68-72]. For top-down process, laser ablation of Si wafer [73-82], electro-chemical etching of Si wafer [83-85] and mechanochemical treatment of bulk Si [86-88] are utilized. The present paper reviewed the above synthesis approaches of Si NPs in the point view of size-controlling and surface functionalization as well as its optical properties.

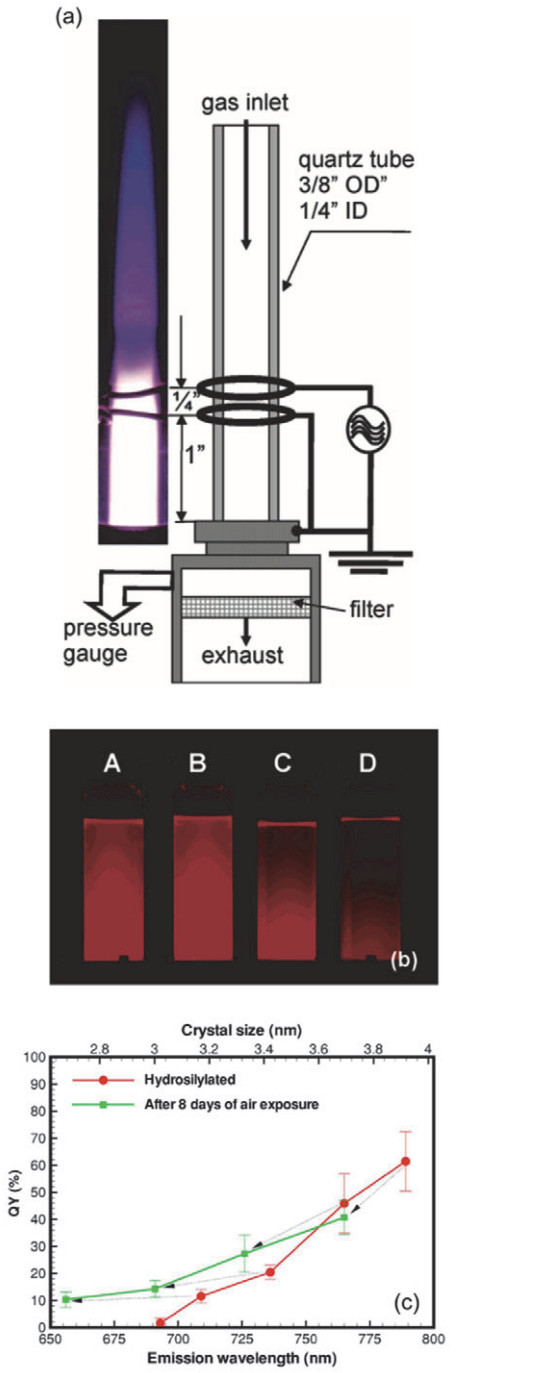

Figure 2. (a) Plasma reactor developed by Kortshagen group and (b) emission of Si NCs synthesized by plasma decomposition (Reprinted with permission from Nano Lett. 2005, 5, 655. Copyright © 2005 American Chemical Society.) (c) QY as a function of Si NCs size and emission wavelength (Reprinted from Appl. Phys. Lett. 88, 233116 (2006), Copyright © 2006 American Institute of Physics).

Plasma decomposition of SiH_4. U. Kortshagen's group initially reported the preparation of Si NPs via plasma decomposition of SiH_4 [37]. By inducing the flow of SiH_4 and argon (Ar) mixture into a non-thermal low-pressure plasma reactor (shown as Figure 2a), different sized Si NCs can be obtained by changing the partial pressure of SiH_4 or the residence time. The average size of primary Si NPs is tuned in 3-6 nm, which emit orange-red PL when excited by a UV lamp at 365 nm (see Figure 2b). Such PL is originated from the inter surface state formed native Si oxide during particle synthesis. By further optimization of experimental condition, Si NCs with size near 4 nm was synthesized, which performs PL at 789 nm with highest quantum yield of 62% ± 11%, as given by Figure 2c. The quantum yield is dramatically decreased when the size of Si NCs is decreased as the PL peak blue-shifted, however, the reason of this phenomenon is not clearly clarified [38].

Chemical reduction of $SiCl_4$. The synthesis of Si NCs via chemical reduction of $SiCl_4$ has been reported by utilizing different reductant chemicals, including zintl salt [42-46], $LiAlH_4$ [47-51] or sodium naphthalide in solution [52-55]. For Zintl salt as reductant, Yang et al. reported the synthesis of crystalline Si NPs under room temperature [42]. The size of Si NPs is 3~4 nm when the length of alkyl termination in Zintl salt is varied, while the PL spectra show similar peak wavelength around 360 nm. As another synthetic routine, Si NPs was prepared via the chemical reduction of $SiCl_4$ with $LiAlH_4$ [47-51]. Hydrogen-terminated Si NPs were firstly observed, whose surface can be further selectively functionalized by alkene [47] or allylamine [48,51] by using Pt catalyst in solution. Despites the above heterogeneous reactions, researchers of Kauzlarich group demonstrated a homogenous reaction between $SiCl_4$ and sodium naphthalenide as a new synthesis routine for high crystalline Si NPs [52]. The synthesized Si NPs perform PL in blue region (λ = 410~430 nm). Interestingly, ultra-stable blue PL was obtained from a siloxane-coated Si NPs through multiple step surface passivation, as indicated in Figure 3a [53]. Such synthesized Si NPs show air oxygen and moisture stable emission when stored in non-polar organic solvent up to one year, as illustrated by Figure 3b. In addition, by using carbazole as surface functionalization group, Wang and coworkers reported the ultrabright PL from Si NPs with a quantum yield of 70 % (see details in Figure 3c and 3d) [54,55].

Thermal pyrolysis of HSQ. In 2006, Hessel and colleges firstly reported the thermal pyrolysis synthesis

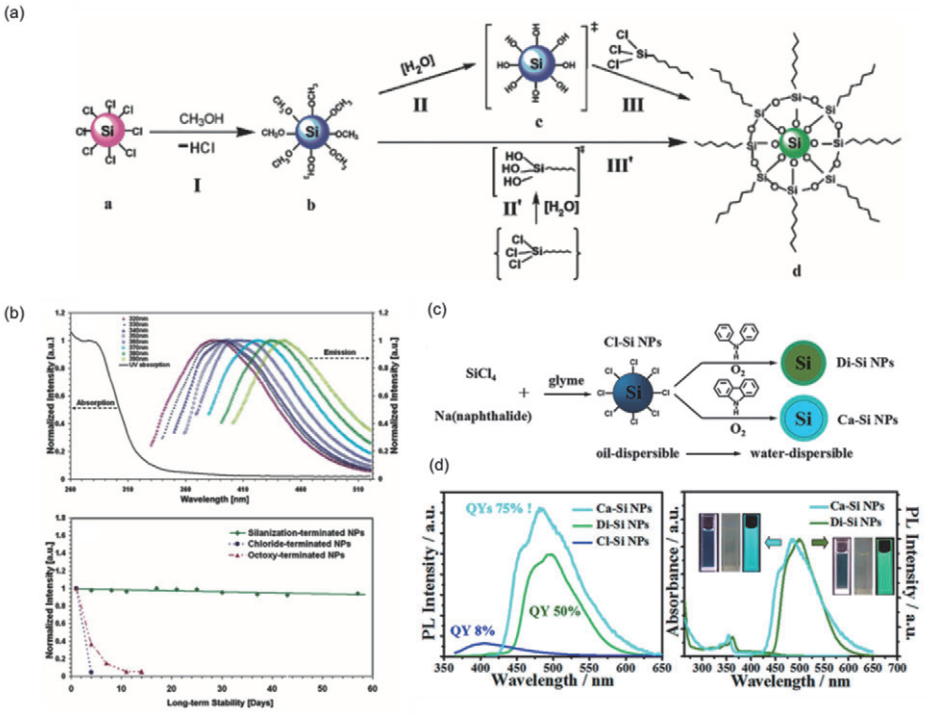

Figure 3. (a) Multiple step surface passivation for siloxane-coated Si NPs and (b) PL and its stability of siloxane-coated Si NCs synthesized by plasma decomposition (Reprinted with permission from Nano Lett. 2004, 4, 1181. Copyright © 2004 American Chemical Society.). (c) synthesis and surface functionalization process and (d) PL and QY of carbozole-capped Si NPs. (Reprinted with permission from J. Am. Chem. Soc. 2013, 135, 14924. Copyright: © 2013 American Chemical Society.).

of nanocrystalline Si-SiO_2 composites and free-standing Si NPs by utilizing HSQ as a novel molecular precursor [56]. Si NPs embedded SiO_2 can be observed by one-hour thermal pyrolysis of HSQ at temperature higher than 500 °C under a mixed insert atmosphere of 4% H_2 and 96% N_2. The nanocrystalline Si NPs with size less than 5 nm can be obtained when the temperature approach to 1000 °C, and the size of Si NCs is increased as the temperature increases to 1400 ° C. With assistance of chemical etching of SiO_2 via HF, the free-standing Si NCs with hydrogen terminated surface can be liberated from matrix composite. The process is illustrated by Figure 4a. The PL maximum peak is shifted in 500-700 nm by changing the period of chemical etching. However, the hydrogen passivated Si NCs is significantly unstable and easily oxides due to the very low disassociation bond energy of Si-H. Efficient surface passivation of different functional groups are achieved through different chemical reactions. Surface passivation of alkyl groups can be induced through hydrosilylation reaction between hydrogen terminated Si NCs and alkene/alkyne under thermal treatment or UV light irradiation [58-61]. Furthermore, Dasog et al. reported the preparation of Si NCs with PL over the visible region by varying the surface functional groups on fix-sized (3-4 nm) hydrogen terminated Si NCs [58]. The PL of synthesized Si NCs covers entire visible wavelength region, and different Si NCs perform excitation wavelength dependent or independent PL, respectively (as given by Figure 4b). Instead of utilizing commercial HSQ as precursor, Xin et al. reported the preparation of photoluminescent Si NCs by thermal pyrolysis of selectively synthesized cross-linked $(HSiO_{1.5})_n$ polymers [62]. The size of Si NCs is controlled in 1-10 nm by thermal pyrolysis at 1100 °C of chemical structure controlled $(HSiO_{1.5})_n$ polymers, whose process avoids the requirement of higher temperature process for size-tuning, as demonstrated by Figure 4c [56,57]. Liberated hydrogen-terminated Si NCs show size dependent PL peaks, ranging from 550 nm to 700 nm.

Thermal disproportionation of SiO. As a commercially available material, SiO is also utilized as a promising precursor for Si NC synthesis through thermal disproportionation reactions [63-66]. Rybaltovskiy et al. previously reported the synthesis of Si/SiOx core/shell nano-particles by thermal disproportionation of SiO, whose process is displayed as Figure 5a [63]. The size of crystalline Si core increases from 4.7 nm to 11.1 nm when the temperature is increased from 350 ºC to 1100 ºC. The synthesized Si/SiOx core/shell nanoparticles and Si NCs perform PL in the infrared wavelength region.

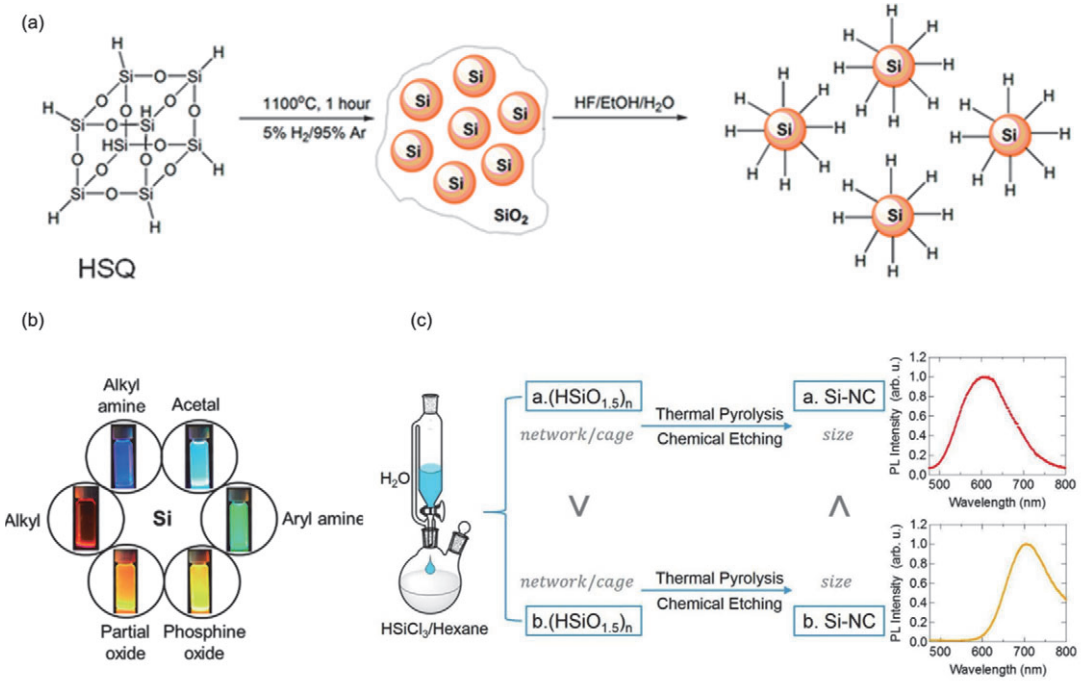

Figure 4. (a) Synthesis of Si NPs by thermal pyrolysis of HSQ and following liberation of Si NPs via chemical etching of HF, and (b) PL images of same sized Si NPs passivated by different functional groups (Reprinted from ACS Nano, 2014, 8(9), 9636-9648. Copyright: © 2014 American Chemical Society.) (c) Size-controlled synthesis of Si NPs by utilizing structure selectively synthesized polymers reported by Xin (Reprinted from Chem. Lett. 2017, 46, 5, 699-702. Copyright: © 2017 The Chemical Society of Japan.).

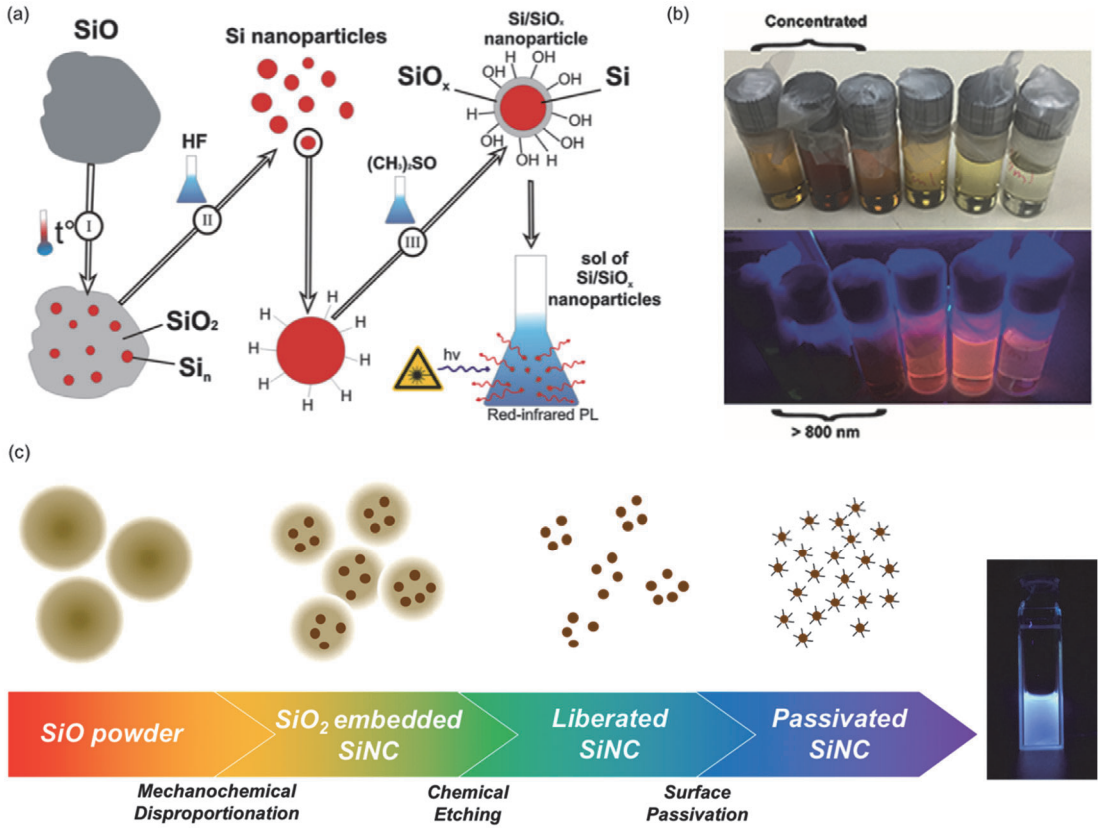

Figure 5. (a) Thermal disproportionation of SiO and preparation of Si/SiOx core/shell NPs (Reprinted from J. Mater. Sci. 2015, 50, 5, 2247-2256. Copyright: © Springer Science+Business Media New York 2014). (b) Infrared and red emission of monodispersed Si NPs fractions separated by size-selective process (Reprinted from Nanoscale, 2016, 8, 3678-3684. Copyright: © The Royal Society of Chemistry 2016). (c) Mechanochemical disproportionation of SiO for synthesis of visible Si NPs (Reprinted from RSC Adv., 2019, 9, 8310. Copyright: © The Royal Society of Chemistry 2019.).

Then, Sun et al. demonstrated the synthesis of free-standing Si NCs on a large-scale, based on thermal disproportionation of SiO at 850–1100 °C. They mentioned that the most significant disproportionation transformations happened in the temperature range between 900 and 950 °C. Based on the original polydisperse Si NCs product, monodisperse Si NCs fractions are selectively separated via a size-selective precipitation. Such liberated Si NCs show corresponding size of 3.5-4 nm with PL wavelength in infrared region around 820-830 nm (Figure 5b) [64].

Mechanochemical disproportionation of SiO. In 2019, Xin et al. reported the synthesis of visible photoluminescent Si NCs via a novel and facile room temperature mechanochemical disproportionation of SiO, whose process is shown in Figure 5c [67]. Compare with the requirement of high temperature (> 900 ºC) in thermal disproportionation process, this new strategy enables room temperature disproportionation via mechanochemical treatment. The size of Si NCs can be easily tuned in 2-5 nm by the duration of mechanochemical treatment, while critical higher temperature (~1400 ºC) is required for size-controlling in the case of thermal disproportionation. In this work, free-standing Si NCs are liberated from the obtained Si-embedded SiO_2 matrix through chemical etching by HF under dark condition. The Si NCs show bright blue PL (λ maximum= 450 nm) after efficient surface passivation of alkyl-group with 1-decene. According to the excitation-wavelength dependent PL, it indicates that the PL of synthesized Si NCs origins from the electron-hole recombination emission on wide bandgap of core state induced from quantum confinement effect, while Si NCs obtained from thermal disproportionation only show PL in infrared region.

Microwave-assisted reductant of APTES. Zhong presents aqueous synthetic approach via in situ growth of Si NPs under microwave irradiation at 160 ºC by utilizing APTES as Si source and trisodium citrate dihydrate as reductant, see details in Figure 6a [68]. This strategy enables large-scale (0.1 g) synthesis in a relatively short time (10 mins). The obtained Si NPs

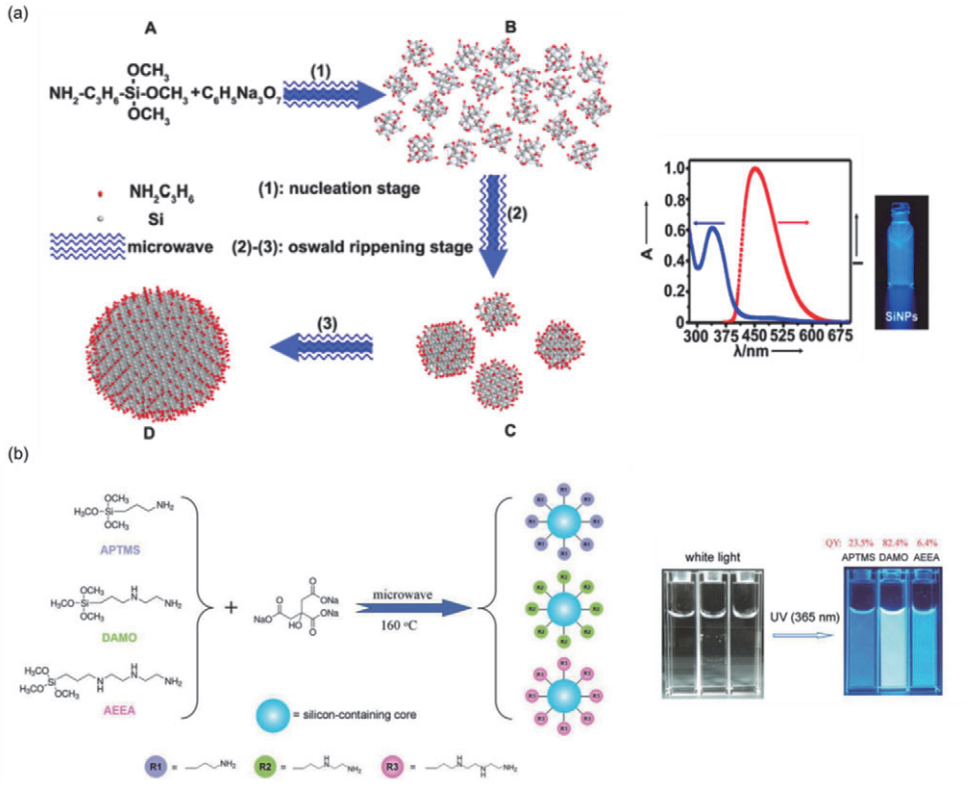

Figure 6. (a) Reaction for microwave-assisted reduction of APTES by trisodium citrate dihydrate and (b) the size distribution, surface chemical groups and PL properties of synthesized Si NPs (Reprinted from J. Am. Chem. Soc. 2013, 135, 8350-8356. Copyright: © 2013 American Chemical Society.). (c) Reactions for Si NPs synthesis via microwave-assisted reduction of different Si precursors and (d) emission from Si NPs when excited by UV light. (Reprinted from Adv. Mater. Interf. 2015, 2, 16, 1500360. Copyright: © 2015 WILEY‐VCH Verlag GmbH & Co. KGaA, Weinheim.).

show average size of 2.2 nm and PL at 450 nm with PL QY up to 20-25 %. As for the surface chemical state, it demonstrates that the obtained Si NPs contains large amount of amino group on surface. By changing the Si source from APTES to N-[3-(trimethoxysilyl) propyl] ethylenediamine (DAMO) and 3-[2-(2-aminoethylamino) ethylamino] propyl-trimethoxysilane (AEEA), the size, surface chemical state, PL properties were investigated in advance [69]. As a result, Si NPs synthesized from DAMO, which exhibits size of 3.4 ± 0.6 and super high QY up to 82.4 % at PL wavelength of 450 nm (as shown in Figure 6b). By replacing the reductant chemical from trisodium citrate dihydrate to glucose, Jo et al. reported a relative low temperature microwave-assisted reaction system [70]. Their prepared Si NPs show Si-Si rich or Si-O rich chemical composition when the reaction temperature changed from 70 ºC to 50 ºC. The observed Si NPs show relatively large size in 5-8nm. Although the PL peak position is quite near to that of Zhong's previous work, the QY is relatively low, 26.2 % for PL at 446 nm. Wu et al. demonstrates the synthesis of dual-color photoluminescent Si NPs via microwave-assisted biomimetic synthetic strategy by utilizing diatom [71]. Red- (3.8 ± 0.8 nm) and blue- (2.1 ± 1.0 nm) emitting Si NPs can be prepared via reaction under 150 ºC for different duration, that is 10 or 180 mins, respectively. Although the QY (15-20 %) is not so high to compare with the previous strategy, the PL show narrower emission spectral width (~30 nm), which indicates a high purity of the PL color saturation. For above strategy, synthesized Si NPs with PL in blue and red region is numerously accomplished. In 2018, Bose et al. prepared green-emitting Si NPs successfully from the microwave-assisted reaction of rice husk in NaOH solution [72]. The diameter of synthesized Si NP is up to 4.9 nm and show green luminescence with a QY of ~60 %.

Laser ablation. Laser ablation has attracted much attention in NPs synthesis due to several advantages, such as 1) facile process such as one-step and one-pot synthesis, 2) NPs with the size of a few nm scale is achieved in short time. Laser ablation has been applied for different target materials in different surroundings. Si NPs have been synthesized via laser ablation in liquid (LAL), inert gas and supercritical fluid, among which

LAL attracts much more attention with respects to the enabled surface passivation along synthesis process [73-82]. As mentioned above, the functional groups on surface not only controls the optical properties of NPs via inducing of surface state, but also affects the solubility of NPs. Liu et al. reported Si NPs with zinc-blende structure is prepared by LAL in water, exhibit size of 7-14 nm and violet-blue PL (λ = 300~440 nm) [73]. The surface of synthesized Si NPs is partially capped with SiO_2, which makes the NPs can be dispersed well in water. On the other hand, Xin et al. reported the synthesis of alkyl-capped visible photoluminescent Si NPs with altered size distributions and optical properties via LAL in several organic solvents with different length of carbon chain [74]. It demonstrates that the average size of Si NPs can be tuned from 1.8 nm to 5.9 nm as the carbon atom ratio in organic solvent is increased. In addition, the absolute QY of Si NPs generated in different solvents show good correlation between size and carbon atom. It worth noting that the synthesized Si NPs show stable PL with enhanced QY during aging in LAL solvent. The above results are summarized as Figure 7. The low yield of NP product is still a challenge due to the limited beam size of laser, although laser ablation is a facile one-step accumulated process with easy size-controlling.

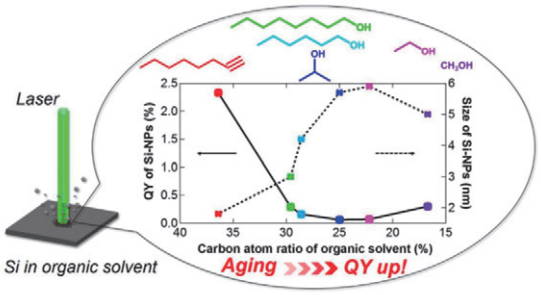

Figure 7. Synthesis of Si NPs via LAL in different organic solvents reported by Xin et al, with the size and QY are correlated as function of carbon atom ratio of organic solvents (Reprinted from Chem. Phys. Lett. 674 (2017) 90-97. Copyright: © 2017 Elsevier B.V. All rights reserved.).

Mechanochemical of bulk Si. Heintz reports blue PL from Si NPs prepared through planetary ball-milling of bulk Si in alkene/alkylene solvents [86]. The synthesized Si NPs surface is simultaneously passivated by stable alkyl/alkenyl groups through mechanochemical treatment, during where the radicals on solvent and surface of bulk Si is covalently linked, such mechanism is described by schematic image given by Figure 8a. The size of Si NPs prepared through 24 hours ball-milling process exhibits size smaller than 4 nm. Synthesized Si NPs show excitation wavelength dependent PL in visible range with wavelength varied in 350-650 nm, as shown in Figure 8b. Dhara el al. demonstrates that the size of Si NCs prepared via the above mechanochemical process can be controlled in 7-20 nm when the ball-milling duration settled from 10-40 hours [88], however, the wide size distribution requires further optimization of experimental condition.

In summary, the size controlling of Si NP can be accomplished by altering the experimental conditions during different process. In the case of plasma of SiH_4, the size was tuned in the range of 2-8 nm by SiH_4 flow rate as well as partial pressure in the Ar mixture. As for the reduction of $SiCl_4$, the size can vary from 1 to 5 nm by changing of reductants and molar ratio of precursor regents. For thermal pyrolysis of HSQ and $(HSiO_{1.5})_n$ (n>8), 4-10 nm sized Si NCs were obtained by changing the temperature of thermal process or the chemical structure of precursor. The size of Si NP produced from laser ablation was 5-8 nm by changing the laser fluences or solvent. As for electrochemical etching of Si wafer, the size was tuned in 2-30 nm by current density and etching time. As for mechanochemical of bulk Si, the NP size was reduced from 20 nm to 7 nm when the milling time was increased from 10 hours to 40 hours. The surface functionalization of Si NPs by different chemical groups has been investigated through different reaction approaches. Most of all, the passivation of alkyl chains has been numerously studied, since a good solubility of Si NPs in nonpolar organic solvent is essential for device fabrication through solution process. In addition, Dohnalova suggested that the alkyl passivation can give rise to the radiative transition rate of Si NP by modifying the electron and hole wavefunctions [30]. The alkyl passivation is mainly conducted on surface-active (dangling-bonds harvested), hydrogen-terminated and halogen-terminated Si NPs. Si NPs with surface-active dangling bonds, prepared by laser ablation or ball milling, they can be directly passivated by alkene or alkyne solvent during high-energy synthesis. For hydrogen-terminated Si NPs, obtained from plasma decomposition or chemical etching, the hydrosilylation has been numerously reported using alkene/alkyne via either thermal-assistant (heating) or photon-assistant (UV laser irradiation). As for halogen-terminated Si NPs, usually obtained from chemical reduction of $SiCl_4$ system, the passivation of

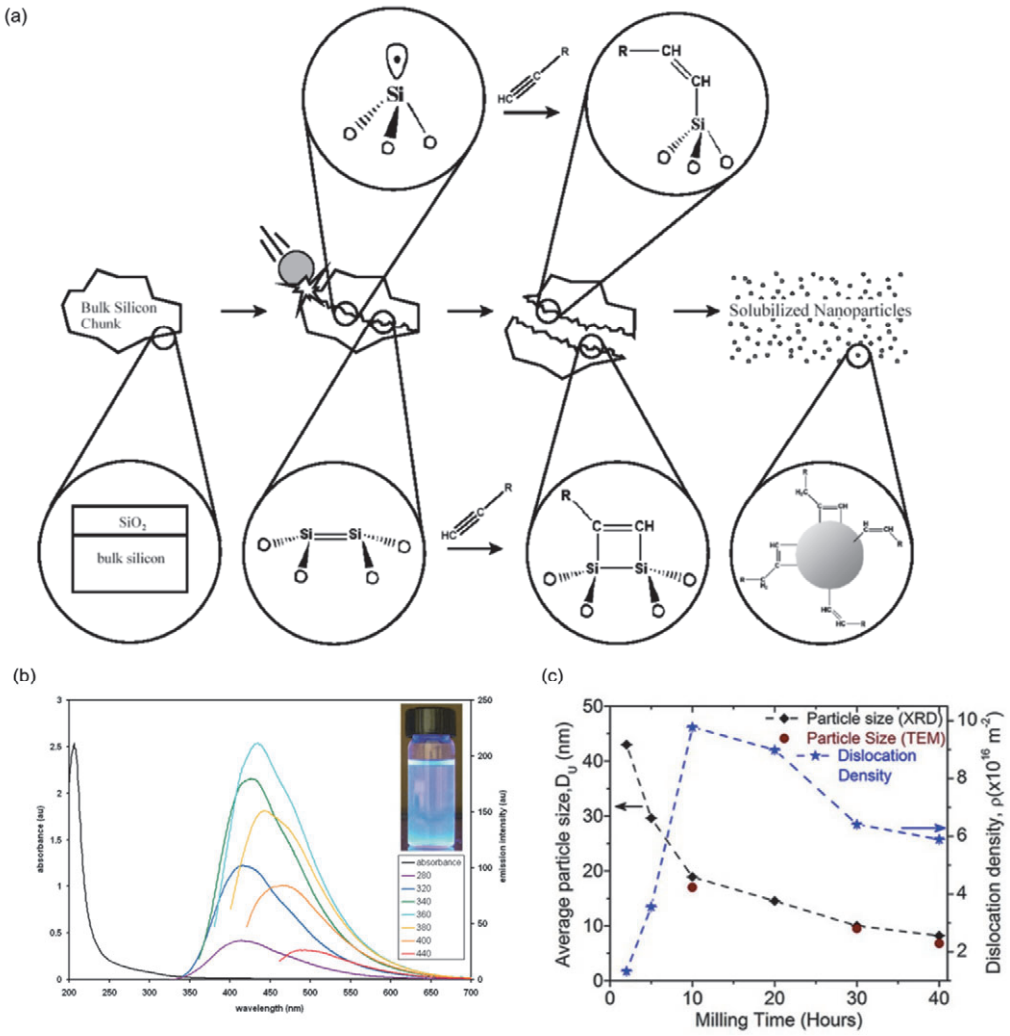

Figure 8. (a) Synthesis mechanism of Si NPs via mechanochemical treatment of bulk Si in alkene solvents. (b) PL spectra and TEM images of obtained Si NPs (Reprinted from Adv. Mater. 2007, 19, 22, 3984-3988. Copyright © 2007 WILEY‐VCH Verlag GmbH & Co. KGaA, Weinheim.). (c) Average size of Si NPs as a function of milling time (Reprinted from Nanoscale Res. Lett. 2011, 6:320. Copyright: © 2011 Dhara and Giri; licensee Springer.).

alkyl chain was induced by chemical reaction with RLi, RMgX and $RSiX_3$ (R=alkyl, X=halogen). The synthesis processes of photoluminescent Si NPs summarized in the present paper might provide good understanding on the size-controlling approaches and surface functionalization, and the related chemical and optical properties are essential for material design of nanomaterials.

Reference

[1] Fox, M. Optical Properties of Solids. *Oxford University Press* 2010.

[2] Haug, H.; Koch, S. W. Quantum Theory of the Optical and Electronic Properties of Semiconductors. *Word Scientific Publishing* 2004.

[3] Harrson, P. Quantum Well, Wires and Dots. *Wiley* 2009.

[4] Pavesi, L.; Turan, R. Silicon Nanocrystals: Fundamentals, Synthesis and Applications. *WILEY-VCH*, 2010.

[5] Khriachtchev, L. Silicon Nanophotonics: Basic Principles, Present Status and Perspectives. *Pan Stanford Publishing* 2008.

[6] Lockwood, D. J. Light Emission in Silicon from Physics to Devices. *Academic Press* 1997.

[7] Kovalev, D.; Heckler, H.; Polisski, G.; Koch, F. Optical Properties of Si Nanocrystals. *Phys. Stat. Sol. (b)* **1999**, *215*, 871.

[8] Dohnalova, K.; Gregorkiewicz, T.; Kusova, K. Silicon Quantum Dots: Surface Matters. *J. Phys.: Condens. Matter* **2014**, *26*, 173201.

[9] Veinot, J. G. C. Synthesis, Surface Functionalization, and Properties of Freestanding Silicon Nanocrystals. *Chem. Commun.* **2006**, 4160.

[10] Cheng, K.-Y.; Anthony, R.; Kortshagen, U. R.; Holmes, R. J. Hybrid Silicon Nanocrystal‐Organic Light-Emitting

Devices for Infrared Electroluminescence. *Nano Lett.* **2010**, *10*, 1154.

[11] Cheng, K.-Y.; Anthony, R.; Kortshagen, U. R.; Holmes, R. J. High-Efficiency Silicon Nanocrystal Light-Emitting Devices. *Nano Lett*. 2011, 11, 1952.

[12] Tu, C.-C.; Tang, L.; Huang, J.; Voutsas, A.; Lin, L. Y. Visible Electroluminescence from Hybrid Colloidal Silicon Quantum Dot-Organic Light-Emitting Diodes. *Appl. Phys. Lett.* **2011**, *98*, 213102.

[13] Puzzo, D. P.; Henderson, E. J.; Helander, M. G.; Wang, Z.; Ozin, G. A.; Lu, Z. Visible Colloidal Nanocrystal Silicon Light-Emitting Diode. *Nano Lett.* **2011**, *11*, 1585.

[14] Maier-Flaig, F.; Rinck, J.; Stephan, M.; Bocksrocker, T.; Bruns, M.; Kubel, C.; Powell, A. K.; Ozin, G. A.; Lemmer, U. Multicolor Silicon Light-Emitting Diodes (SiLEDs). *Nano Lett.* **2013**, *13*, 475.

[15] Ghosh, B.; Masuda, Y.; Wakayama, Y.; Imanaka, Y.; Inoue, J.; Hashi, K.; Deguchi, K.; Yamada, H.; Sakka, Y.; Ohki, S.; Shimizu, T.; Shirahata, N. Hybrid White Light Emitting Diode Based on Silicon Nanocrystals. *Adv. Funct. Mater.* **2014**, *24*, 7151.

[16] Xin, Y.; Nishio, K.; Saitow, K. White-Blue Electroluminescence from a Si Quantum Dot Hybrid Light-Emitting Diode. *Appl. Phys. Lett*. **2015**, *106*, 201102.

[17] Yao, L.; Yu, T.; Ba, L.; Meng H.; Fang, X.; Wang, Y.; Li, L.; Rong, X.; Wang, S.; Wang, X.; Ran, G.; Pi, X.; Qin, G. Efficient Silicon Quantum Dots Light Emitting Diodes with an Inverted Device Structure. *J. Mater. Chem. C.* **2016**, *4*, 673.

[18] Kim, S.-K.; Cho, C.-H.; Kim, B.-H.; Park, S.-J.; Lee, J. W. Electronical and Optical Characteristics of Silicon Nanocrystal Solar Cells. *Appl. Phys. Lett.* **2009**, *95*, 143120.

[19] Priolo, F.; Gregorkiewicz, T.; Galli, M.; Krauss, T. F. Silicon Nanostructures for Photonics and Photovoltaics. *Nat. Nanotech.* **2014**, *9*, 19.

[20] Wright, M.; Uddin, A. Organic-Inorganic Hybrid Solar Cells: A Comparative Review. *Solar Energy Materials & Solar Cells* **2012**, *107*, 87.

[21] Liu, C.-Y.; Kortshagen, U. R. Hybrid Solar Cells from MDMO-PPV and Silicon Nanocrystals. *Nanoscale*, **2012**, *4*, 3963.

[22] Meinardi, F.; Ehrenberg, S.; Dhamo L.; Carulli, F.; Mauri, M.; Bruni, F.; Simonutti, R.; Kortshagen, U.; Brovelli, S. Highly Efficient Luminescent Solar Concentrators Based on Earth-Abundant Indirect-Bandgap Silicon Quantum Dots. Nature Photon. DOI: 10.1038/NPHOTON.2017.5

[23] Conibeer, G.; Grenn, M.; Corkish, R.; Cho, Y.; Cho, E.-C.; Jiang, C.-W.; Fangsuwannarak, T.; Pink, E.; Huang, Y.; Puzzer, T.; Trupke, T.; Richards, B.; Shalav, A.; Lin, K.-L. Silicon Nanostructures for Third Generation Photovoltaic Solar Cells. *Thin Solid Films* **2006**, *511-512*, 654.

[24] Wang, J.; D.-X. Ye, G.-H. Liang, J. Chang, J.-K. Kong anf J.-Y. Chen, One-step synthesis of water-dispersible silicon nanoparticles and their use in fluorescence lifetime imaging of living cells, *J. Mater. Chem. B*, 2, 4338 (2014)

[25] Zhong, Y.; Peng, F.; Bao, F.; Wang, S.; Ji, X.; Yang, L.; Su, Y.; Lee, S.-T.; He, Y. Large-Scale Aqueous Synthesis of Fluorescent and Biocompatible Silicon Nanoparticles and Their Use as Highly Photostable Biological Probes. *J. Am. Chem. Soc.* **2013**, *135*, 8350.

[26] McVey, B. F. P.; Tilley, R. D. Solution Synthesis, Optical Properties, and Bioimaging Applications of Silicon Nanocrystals. *Acc. Chem. Res.* **2014**, *47*, 3045.

[27] Das, P.; Saha, A.; Maity, A. R.; Ray, S. C.; Jana, N. R. Silicon Nanoparticle Based Fluorecent Biological Label via Low Temperature Thermal Degradation of Chloroalkylsilane. *Nanoscale* **2013**, *5*, 5732.

[28] Fan, J.; Chu, P. K. Group IV Nanoparticles: Synthesis, Properties, and Biological Applications. *Small*, **2010**, *6*, 2080.

[29] Canham, L. T. Silicon Quantum Wire Array Fabrication by Electrochemical and Chemical Dissolution of Wafers. *Appl. Phys. Lett.* **1990**, *57*, 1046.

[30] Dohnalva, K.; Poddubny, A. N.; Prokofiev, A. A.; DAM de Boer, W.; Umesh, C. P.; Paulusse, J. M. J.; Zuihof, H.; Gre, T. Surface Brightens Up Si Quantum Dots: Direct Bandgap-Like Size-Tunable Emission. *Light Sci. Appl.* **2013**, *2*, e47.

[31] Hapala, P.; Kusova, K.; Pelant, I.; Jelinek, P. Theoretical Analysis of Electronic Band Structure of 2- to 3-nm Si Nanocrystals. *Phys. Rev. B* **2013**, *87*, 195420.

[32] Ledoux, G.; Guillois, O.; Porterat, D.; Reynaud, C. Photoluminescence Properties of Silicon Nanocrystals as a Function of Their Size. *Phys. Rev. B* **2000**, *62*, 15942.

[33] Barbagiovanni, E. G.; Goncharova, L. V.; Simpson, P. J. Electronic Structure Study of Ion-Implanted Si Quantum Dots in a SiO_2 Matrix: Analysis of Quantum Confinement Theories. *Phys. Rev. B* **2011**, *83*, 035112.

[34] Gali, A.; Voros, M.; Rocca, D.; Zimanyi, G. T.; Galli, G. High-Energy Excitations in Silicon Nanoparticles. *Nano Lett.* **2009**, *9*, 3780.

[35] Khriachtchev, L.; Ossicini, S.; Iacona, F.; Gourbilleau, F. Silicon Nanoscale Materials: From Theoretical Simulations to Photonic Applications. *Inter. J. Photoenergy* **2012**, *2012*, Article ID872576.

[36] Godefroo, S.; Hayne, M.; Jivanescu, M.; Stesmans, A.;

Zacharias, M.; Lebedev, O. I.; Van Tendeloo, G.; Moshchalkov, V. V. Classification and Control of the Origin of Photoluminescence from Si Nanocrystals. *Nat. Nanotech.* **2008**, *3*, 174.

[37] Mangolini, L.; Thimsen, E.; Kortshagen, U. High-Yield Plasma Synthesis of Luminescent Silicon Nanocrystals. *Nano Lett.* **2005**, *5*, 655.

[38] Jurbergs, D.; Rogojina, E.; Mangolini, L.; Kortshagen, U. Silicon Nanocrystals with Ensemble Quantum Yields exceeding 60 %. *Appl. Phys. Lett.* **2006**, *88*, 233116.

[39] Kortshagen, U. Nonthermal Plasma Synthesis of Nanocrystals: Fundamentals, Applications, and Future Research Needs. *Plasma Chem. Plasma Process* **2016**, *36*, 73.

[40] Gupta, A.; Swihart, M.; Wiggers, H. Luminescent Colloidal Dispersion of Silicon Quantum Dots from Microwave Plasma Synthesis: Exploring the Photoluminescence Behavior across the Visible Spectrum. *Adv. Funct. Mater.* **2009**, *19*, 696.

[41] Gupta, A.; Wiggers, H. Freestanding Silicon Quantum Dots: Origin of Red and Blue Luminescenec. *Nanotechnology*, **2011**, *22*, 055707.

[42] Yang, C.-S.; Bley, R. A.; Kauzlarich, S. M.; Lee, H. W. H.; Delgado, G. R. Synthesis of Alkyl-Terminated Silicon Nanoclusters by a Solution Route. *J. Am. Chem. Soc.* **1999**, *121*, 5191.

[43] Dohnalova, K.; Fucikova, A.; Umesh, C. P.; Humpolickova, J.; Paulusse, J. M.; Valenta, J.; Zuilhof, H.; Hof, M.; Gregorkiewicz, T. Microscopic Origin of the Fast Blue-Green Luminescence of Chemically Synthesized Non-oxidized Silicon Quantum Dots. *Small* **2012**, *8*, 3185.

[44] Valenta, J.; Fucikova, A.; Pelant, I.; Dohnalova, K.; Aleknavicius, A.; Cibulka, O.; Fojtik, A.; Kada, G. On the Origin of the Fast Photoluminescence Band in Small Silicon Nanoparticles. *New J. Phys.* **2008**, *10*, 073022.

[45] Mayeri, D.; Phillips, Brian L.; Augustine, M. P.; Kauzlarich, S. M. NMR Study of the Synthesis of Alkyl-Terminated Silicon Nanoparticles from the Reaction of $SiCl_4$ with the Zintl Salt, NaSi. *Chem. Mater.* **2001**, *13*, 765.

[46] Pettigrew, K. A.; Liu, Q.; Power, P. P.; Kauzlarich, S. M. Solution Synthesis of Alkyl- and Alkyl/Alkoxy-Capped Silicon Nanoparticles via Oxidation of Mg_2Si. *Chem. Mater.* **2003**, *15*, 4005.

[47] Warner, J. H.; Hoshino, A.; Yamamoto, K.; Tilley, R. D. Water-Soluble Photoluminescent Silicon Quantum Dots. *Angew. Chem. Int. Ed.* **2005**, *44*, 4550.

[48] Tilley, R. D.; Warner, J. H.; Yamamoto, K.; Matsui, I.; Fujimori, H. Micro-Emulsion Synthesis of Monodisperse Surface Stabilized Silicon Nanocrystals. *Chem. Commun.* **2005**, 1833.

[49] Portolles, M. J. L.; Diez, R. P.; Dell'Arciprete, M. L.; Caregnao, P.; Romero, J. J.; Martire, D. O.; Azzaroni, O.; Ceolin, M.; Gonzalez, M. C. Understanding the Parameters Affecting the Photoluminescence of Silicon Nanoparticles. *J. Phys. Chem. C* **2012**, *116*, 11315.

[50] Chatterjee, S. Mukherjee, T. K. Size-Dependent Differential Interaction of Allylamine-Capped Silicon Quantum Dots with Surfactant Assemblies Studied Using Photoluminescence Spectroscopy and Imaging Technique. *J. Phys. Chem. C.* **2013**, *117*, 10799.

[51] Rosso-Vasic, M.; Spruiji, E.; Van Lagen, B.; De Cola, L.; Zuilhof, H. Alkyl-Functionalized Oxide-Free Silicon Nanoparticles: Synthesis and Optical Properties. *Small* **2008**, *4*, 1835.

[52] Baldwin, R. K.; Pettigrew, K. A.; Ratai, E.; Augustine, M. P.; Kauzlarich, S. M. Solution Reduction Synthesis of Surface Stabilized Silicon Nanoparticles. *Chem. Commun.* **2002**, 1822.

[53] Zou, J.; Baldwin, R. K.; Pettigrew, K. A.; Kauzlarich, S. M. Solution Synthesis of Ultrastable Luminescent Siloxane-Coated Silicon Nanoparticles. *Nano Lett.* **2004**, *4*, 1181.

[54] Li, Q.; He, Y.; Chang, J.; Wang, L.; Chen, H.; Tan, Y.; Wang, H.; Shao, Z. Surface-Modified Silicon Nanoparticles with Ultrabright Photoluminescence and Single-Exponential Decay for Nanoscale Fluorescence Lifetime Imaging of Temperature. *J. Am. Chem. Soc.* **2013**, *135*, 14927.

[55] Wang, L.; Li, Q.; Wang, H; Huang, J.; Zhang, R.; Chen, Q.; Xu, H.; Han, W.; Shao, Z.; Sun, H. Ultrafast Optical Spectroscopy of Surface-modified Silicon Quantum Dots: Unraveling the Underlying Mechanism of the Ultrabright and Color-tunable Photoluminescence. *Light Sci. Appl.* **2015**, *4*, e245.

[56] Hessel, C. M.; Henderson, E. J.; Veinot, J. G. C. Hydrogen Silsesquioxane: A Molecular Precursor for Nanocrystalline Si-SiO_2 Composites and Freestanding Hydride-Surface-Terminated Silicon Nanoparticles. *Chem. Mater.* **2006**, *18*, 6139.

[57] Hessel, C. M.; Kelly, J. A.; Veinot, J. G. C. Influence of $HSiO_{1.5}$ Sol-Gel Polymer Structure and Composition on the Size and Luminescent Properties of Silicon Nanocrystals. *Chem. Mater.* **2009**, *21*, 5426.

[58] Dasog, M.; De los Reyes, G. B.; Titova, L. V.; Hegmann, F. A.; Veinot, J. G. C. Size vs Surface: Tuning the Photoluminescence of Freestanding Silicon Nanocrystals across the Visible Spectrum via Surface Groups. *ACS Nano* **2014**, *8*, 9636.

[59] Nunez, J. R. R.; Kelly, J. A.; Henderson, E. J.; Veinot, J. G. C. Synthesis of Ligand-Stabilized Silicon Nanocrystals with Size-Dependent Photoluminescence Spanning Visible to Near-Infrared Wavelengths. *Chem. Mater.* **2012**, *24*, 393.

[60] Mastronardi, M. L.; Maier-Flaig, F.; Faulkner, D.; Henderson, E. J.; Kubel, C.; Lemmer, U.; Ozin, G. A. Size-Dependent Absolute Quantum Yields for Size-Separated Colloidally-Stable Silicon Nanocrystals. *Nano Lett.* **2012**, *12*, 337.

[61] Hessel, C. M.; Reid, D.; Panthani, M. G.; Rasch, M. R.; Goodfellow, B. W.; Wei, J.; Fujii, H.; Akhavan, V.; Korgel, B. A. Synthesis of Ligand-Stabilized Silicon Nanocrystals with Size-Dependent Photoluminescence Spanning Visible to Near-Infrared Wavelengths. *Chem. Mater.* **2012**, *24*, 393.

[62] Xin, Y.; Wakimoto, R.; Saitow, K. Synthesis of Size-Controlled Luminescent Si Nanocrystals from $(HSiO_{1.5})_n$ Polymers. *Chem. Lett.* **2017**, *46*, 699.

[63] Rybaltovskiy, A. O.; Ischenko, A. A.; Zavorotny, Y. S.; Garshev, A. V.; Dorofeev, S. G.; Kononov, N. N.; Minaev, N. V.; Minaeva, S. A.; Sviridoc, A. P.; Timashev, P. S.; Khodos, I. I.; Yusupov, V. I.; Lazov, M. A.; Panchenoko, V. Y. A.; Bagratashvili, V. N. Synthesis of Photoluminescent Si/SiOx Core/shell Nanoparticles by Thermal Disproportionation of SiO: Structural and Spectral Characterization. *J. Mater. Sci.* **2015**, *50*, 2247.

[64] Sun, W.; Qian, C.; Cui, X. S.; Wang, L.; Wei, M.; Casillas, G. A.; Helmy, S.; Ozin, G. A. Silicon Monoxide-A Convenient Precursor for Large Scale Synthesis of Near Infrared Emitting Monodisperse Silicon Nanocrystals. *Nanoscale* **2016**, *8*, 3678.

[65] Sun, W.; Qian, C.; Wang, L.; Wei, M.; Mastronardi, M. L.; Casilla, G.; Breu, J.; Ozin, G. A. Switching-on Quantum Size Effects in Silicon Nanocrystals. *Adv. Mater.* **2015**, *27*, 746.

[66] Dorofeev, S. G.; Ishchenko, A. A.; Kononov, N. N.; Fetisov, G. V. Effect of Annealing Temperature on the Optical Properties of Nanosilicon Produced from Silicon Monoxide. *Curr. Appl. Phys.* **2012**, *12*, 718.

[67] Xin, Y.; Xu, Y.; Lee, J.; Shirai, T. A Novel and Facile Synthesis of Visible Photoluminescence of Si Nanocrystals by Room Temperature Mechanochemical Disproportionation of SiO. *RSC Adv.* **2019**, *9*, 8310.

[68] Zhong, Y.; Peng, F.; Bao, F.; Wang, S.; Ji, X.; Yang, L.; Su, Y.; Lee, S.-T.; He, Y. Large-Scale Aqueous Synthesis of Fluorescent and Biocompatible Silicon Nanoparticles and Their Use as Highly Photostable Biological Probes. *J. Am. Chem. Soc.* **2013**, *135*, 8350.

[69] Wu, F.-G.; Zhang, X.; Kai, S.; Zhang, M.; Wang, H.-Y.; Myers, J. N.; Weng, Y.; Liu, P.; Gu, N.; Chen, Z. One-Step Synthesis of Superbright Water-Soluble Silicon Nanoparticles with Photoluminescence Quantum Yield Exceeding 80%. *Adv. Mater. Interfaces* **2015**, *2*, 1500360.

[70] Jo, S.; Ryu, B.; Chae, A.; Choi, Y.; Kang, E. B.; Nur'aeni; Park, B.; Park,S. Y.; In, Insik. Microwave-assisted Synthesis of Highly Fluorescent and Biocompatible Silicon Nanoparticles Using Glucose as Dual Roles of Reducing Agents and Hydrophilic Ligands. *Chem. Lett.* **2017**, *46*, 398.

[71] Wu, S.; Zhong, Y.; Zhou, Y.; Song, B.; Chu, B.; Ji, X.; Wu, Y.; Su, Y.; He, Y. Biomimetic Preparation and Dual-Color Bioimaging of Fluorescent Silicon Nanoparticles. *J. Am. Chem. Soc.* **2015**, *137*, 14726.

[72] Bose, S.; Ganayee, M. A.; Mondal, B.; Baidya, A.; Chennu, S.; Mohanty, J. S.; Pradeep, T. Synthesis of Silicon Nanoparticles from Rice Husk and their Use as Sustainable Fluorophores for White Light Emission. *ACS Sustainable Chem. Eng.* **2018**, *6*, 6203.

[73] Liu, P.; Liang, Y.; Li, H. B.; Xiao, J.; He, T.; Yang, G. W. Violet-Blue Photoluminescence from Si Nanoparticles with Zinc-Blende Structure Synthesized by Laser Ablation in Liquids. *AIP Adv.* **2013**, *3*, 022127.

[74] Svrcek, V.; Sasaki, T.; Shimizu, Y.; Koshizaki, N. Blue Luminescent Silicon Nanocrystals Prepared by ns Pulsed Laser Ablation in Water. *Appl. Phys. Lett.* **2006**, *89*, 213113.

[75] Alkis, S.; Okyay, A. K.; Ortac, B. Post-Treatment of Silicon Nanocrystals Produced by Ultra-Short Pulsed Laser Ablation in Liquid: Toward Blue Luminescent Nanocrystal Generation. *J. Phys. Chem. C* **2012**, *116*, 3432.

[76] Shirahata, N.; Linford, M. R.; Furumi, S.; Pei, L.; Sakka, Y.; Gates, R. J.; Asplund, M. C. Laser-Derived One-Pot Synthesis of Silicon Nanocrystals Terminated with Organic Monolayers. *Chem. Commun.* **2009**, *31*, 4684.

[77] Dewan, S.; Odhner, J. H.; Tibbetts, K. M.; Afsari, S.; Levis, R. J.; Borguet, E. Resolving the Source of Blue Luminescence from Alkyl-capped Silicon Nanoparticles Synthesized by Laser Pulse Ablation. *J. Mater. Chem. C* **2016**, *4*, 6894.

[78] Tan, D.; Ma, Z.; Xu, B.; Dai, Y.; Ma, G.; He, M.; Jin, Z.; Qiu, J. Surface Passivated Silicon Nanocrystals with Stable Luminescence Synthesized by Femtosecond Laser Ablation in Solution. *Phys. Chem. Chem. Phys.* **2011**, *13*, 20255.

[79] Xin, Y.; Kitasako, T.; Maeda, M.; Saitow, K. Solvent Dependence of Laser-Synthesized Blue-Emitting Si Nanoparticles: Size, Quantum Yield, and Aging

Performance. *Chem. Phys. Lett.* **2017**, *674*, 90.

[80] Saitow, K. Silicon Nanoclusters Selectively Generated by Laser Ablation in Supercritical Fluid. *J. Phys. Chem. C* **2005**, *109*, 3731.

[81] Saitow, K.; Yamamura, T. Effective Cooling Generates Efficient Emission: Blue, Green, and Red Light-Emitting Si Nanocrystals. *J. Phys. Chem. C* **2009**, *113*, 8465.

[82] Wei, S.; Yamamura, T.; Kajiya, D.; Saitow, K. White-Light-Emitting Silicon Nanocrystal Generated by Pulsed Laser Ablation in Supercritical Fluid: Investigation of Spectral Components as a Function of Excitation Wavelengths and Aging Time. *J. Phys. Chem. C* **2012**, *116*, 3928.

[83] Kang, Z.; Liu, Y.; Tsang, C. H. A.; Duo Duo Ma, D.; Fan, X.; Wong, N.-B.; Lee, S.-T. Water-Soluble Silicon Quantum Dots with Wavelength-Tunable Photoluminescence. *Adv. Mater.* **2009**, *21*, 661.

[84] Tu, C.; Tang, L.; Huang, J.; Voutsas, A.; Lin, L. Y. Solution-Processed Photodetectors from Colloidal Silicon Nano/Micro Particle Composite. *Opt. Express* **2010**, *18*, 21622.

[85] Secret, E.; Leonard, C.; Kelly, S. J.; Uhl, A.; Cozzan, C.; Andrew, J. S. Size Control of Porous Silicon-Based Nanoparticles via Pore-Wall Thinning. *Langmuir* **2016**, *32*, 1166.

[86] Heintz, A. S.; Fink, M. J.; Mitchell, B. S. Mechanochemical Synthesis of Blue Luminescent Alkyl/Alkenyl-Passivated Silicon Nanoparticles. *Adv. Mater.* **2007**, *19*, 3984.

[87] Heintz, A. S.; Fink, M. J.; Mitchell, B. S. Silicon Nanoparticles with Chemically Tailored Surface. *Appl. Organometal. Chem.* **2010**, *24*, 236.

[88] Dhara, S.; Giri, PK. Size-Dependent Visible Absorption and Fast Photoluminescence Decay Dynamics from Freestanding Strained Silicon Nanocrystals. *Nanoscale Res. Lett.* **2011**, *6*, 320.